Escherichia coli Aspartate Transcarbamylase: The Relation Between Structure and Function

EVAN R. KANTROWITZ AND WILLIAM N. LIPSCOMB

The x-ray structures of the allosteric enzyme aspartate transcarbamylase from *Escherichia coli* have been solved and refined for both allosteric forms. The T form was determined in the presence of the heterotropic inhibitor cytidine triphosphate, CTP, while the R form was determined in the presence of the bisubstrate analog *N*-phosphonacetyl-L-aspartate. These two x-ray structures provide the starting point for an understanding of how allosteric enzymes are able to control the rates of metabolic pathways. Insights into the mechanisms of both catalysis and homotropic cooperativity have been obtained by using site-directed mutagenesis to probe residues thought to be critical to the function of the enzyme based on these x-ray structures.

ASPARTATE TRANSCARBAMYLASE OF *Escherichia coli* [E.C. 2.1.3.2] is a member of a special class of enzymes that not only catalyzes a cellular reaction, but also controls the rate of a metabolic pathway. The enzymes in this class are usually large, each composed of more than one polypeptide chain, and catalyze a reaction at or near the beginning of a metabolic pathway. Aspartate transcarbamylase catalyzes the condensation of carbamyl phosphate with L-aspartate to produce *N*-carbamyl-L-aspartate and inorganic phosphate (*1*). This reaction is particularly important because once carbamylaspartate is formed, it is committed to the biosynthesis of pyrimidines, a necessary component for nucleic acid biosynthesis. Aspartate transcarbamylase controls the rate of pyrimidine biosynthesis by altering its catalytic velocity in response to cellular levels of both pyrimidines and purines. The end product of the pyrimidine pathway, CTP, induces a decrease in catalytic velocity, whereas adenosine triphosphate (ATP), the end product of the parallel purine pathway, exerts the opposite effect, stimulating the catalytic activity (*2*). In part, the relative amounts of purines and pyrimidines in the cell are thereby kept in balance for nucleic acid synthesis. By using x-ray crystallography and site-directed mutagenesis we have begun to delineate on the molecular level how this complex enzyme catalyzes the formation of carbamylaspartate and how it alters its catalytic activity in response to cellular metabolites.

Aspartate transcarbamylase is composed of 12 polypeptide chains of two types. Each of the six larger, or catalytic, chains (C1 through C6) has a molecular weight of 33,000, and they are grouped together in two trimers (Fig. 1). Each of the smaller, or regulatory, chains (R1 through R6), has a molecular weight of 17,000 and they are organized in three dimers (Fig. 1). The packing of the two catalytic trimers (catalytic subunits) and the three regulatory dimers (regulatory subunits) results in a highly symmetric molecule with D_3 symmetry.

The holoenzyme can be dissociated into the catalytic and regulatory subunits that can easily be isolated (*3*). Furthermore, the holoenzyme can be reconstituted from the separate subunits under appropriate conditions. Only the isolated catalytic subunits have enzymatic activity (*4*). The isolated regulatory subunits bind the nucleotide effectors ATP and CTP. A comparison of the kinetics of the catalytic subunit and the holoenzyme reveals two important differences. First, the specific activity of the catalytic subunit is about 50% higher than that of the holoenzyme; and second, the substrate saturation curves change from sigmoidal for the holoenzyme to hyperbolic for the catalytic subunit.

A sigmoidal substrate saturation curve is a characteristic of the class of enzymes that exert allosteric control of biosynthetic pathways. Over a very narrow concentration range these enzymes are capable of substantial alterations in their catalytic ability. These sigmoidal saturation curves imply interacting sites, where the binding of the first substrate induces changes in substrate affinity or catalytic efficiency or both at the other, sometimes distant active sites. Both the Monod, Wyman, and Changeux (*5*) and the Koshland, Nemethy, and Filmer (*6*) models require two alternate states of the enzyme, which have often been called the T and R states. The T state has lower affinity for substrate and lower activity than does the R state (*7*).

For aspartate transcarbamylase, the R state can be induced by the substrates as well as by certain substrate analogs such as *N*-phosphonacetyl-L-aspartate (PALA), which resembles the natural substrates carbamyl phosphate and aspartate (*8*) (see Fig. 2). Either PALA or a combination of carbamyl phosphate and succinate, an analog of aspartate, can convert the enzyme from the T state to the R state. This conversion has been monitored, for example, by ultraviolet difference spectroscopy (*8, 9*), difference sedimentation (*10*), circular dichroism (*11*), and x-ray solution scattering (*12*). It became clear from the single-crystal x-ray diffraction studies (*13–15*) that contraction of the catalytic subunits when PALA binds to the holoenzyme involved movements of as much as 13 Å during closure of the active sites, and that the T to R transition involved an expansion along the molecular threefold axis by 12 Å, as we now describe.

Structure of the Enzyme

High-resolution structures are known from the unligated enzyme (*13*), the CTP enzyme (*14*), and the PALA enzyme (*15*). One regulatory-catalytic (RC) unit is shown in Fig. 3, where the location

E. R. Kantrowitz is at the Department of Chemistry, Boston College, Chestnut Hill, MA 02167. W. N. Lipscomb is at the Gibbs Laboratory, Harvard University, 12 Oxford Street, Cambridge, MA 02138.

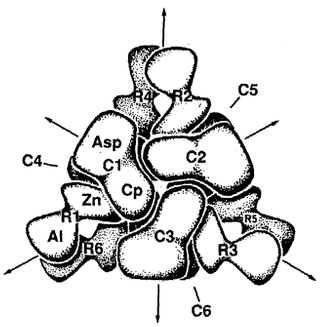

Fig. 1. Schematic representation of the quaternary structure of aspartate transcarbamylase viewed along the threefold axis. The six catalytic (C) and regulatory (R) chains are numbered. Catalytic chains C1–C2–C3 and C4–C5–C6 correspond to the two catalytic subunits, whereas the regulatory chains R1–R6, R2–R4, and R3–R5 correspond to the three regulatory subunits. The catalytic chain is composed of the aspartate (Asp) and the carbamyl phosphate (Cp) domains. The regulatory chain is composed of the allosteric (Al) and zinc (Zn) domains. The arrows indicate the molecular twofold axes.

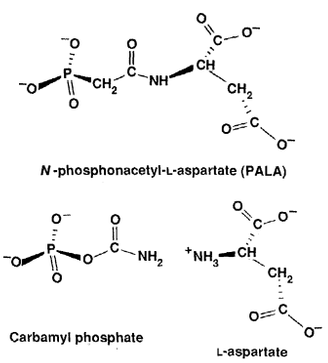

Fig. 2. Structures of the two substrates of aspartate transcarbamylase, carbamyl phosphate, and L-aspartate, along with the bisubstrate analog, *N*-phosphonacetyl-L-aspartate (PALA) (*8*).

of PALA is indicated between the carbamyl phosphate domain (light green) and the aspartate domain (blue) of the catalytic chain in the R structure. The structural (noncatalytic) Zn^{2+} ion is shown in the zinc domain (red), and the CTP site is added to the allosteric domain (yellow) from the T form to this R structure of the regulatory chain. As shown in Fig. 1, the two catalytic trimers stack upon one another along the molecular threefold axis in a nearly eclipsed configuration. Each regulatory dimer joins two catalytic chains that are in different C_3 units and that are rotated ~120° about the threefold axis, for example, C1–R1–R6–C6 (Fig. 1).

Each catalytic chain contains one active site near the interface between adjacent catalytic chains in a C_3 unit. Residues required for maximal activity are contributed by these adjacent pairs of catalytic chains. These shared active sites have recently been demonstrated with the use of hybrid subunits in the holoenzyme (*16*). The six active sites face a central cavity, which is readily accessible from the outside of the molecule in both the T and R forms.

The structure of the PALA-ligated enzyme shows interactions of PALA with Ser^{52}, Thr^{53}, Arg^{54}, Thr^{55}, Arg^{105}, His^{134}, Arg^{167}, Arg^{229}, Gln^{231}, and Leu^{267} from one catalytic chain and Ser^{80} and Lys^{84} from the adjacent catalytic chain (Fig. 4). Thus major interactions occur between the negative charges of PALA and five positively charged residues of the enzyme. When PALA is displaced by carbamyl phosphate plus succinate (*17*), the terminal oxygens of carbamyl phosphate and of the carboxylate groups of succinate are near those in the PALA enzyme. Also, the plane of the amide group of carbamyl phosphate is almost perpendicular to the plane of the peptide-like bond of PALA. In this region, interactions of main-chain carbonyls of Pro^{266} and Leu^{267} and the side-chain carbonyl of Gln^{137} occur with the primary carbamyl nitrogen. Also, the carbonyl oxygen of carbamyl phosphate interacts with Thr^{55}, Arg^{105}, and His^{134}, and the mixed anhydride oxygen of carbamyl phosphate interacts with Arg^{54}. In a later section we consider the effects of site-specific mutagenesis on many of these interactions. Here, we note that PALA seems to be a good analog for carbamyl phosphate and succinate. If a primary amino group is added to succinate to make aspartate, we have a model of an important step: this amino group is in a position to attack the carbonyl carbon of carbamyl phosphate perpendicular to the plane of the carbamyl group. From the purely structural view, the removal of a proton from this attacking amino group is ambiguous in this model and could be accomplished by His^{134}, a phosphate oxygen, or a water molecule as an intermediate transfer agent.

The major change in tertiary structure induced by the binding of PALA or substrate analog is the α-carbon movement of up to 8 Å of the 240s loop (residues 225 to 245). The accompanying closure at the active site is about 2 Å (residues 50 to 55). In addition, movements of about 5 Å are seen in the α-carbon movements of residues 70 to 75, which are associated with the split active site.

These changes in tertiary structure cause a large change in the quaternary structure (Fig. 5). As the T form is converted to the R form by binding of substrate analog, the two C_3 units move apart by 12 Å, and reorient about the molecular threefold axis by ±5° (a relative reorientation of 10°). Also, the regulatory dimers reorient about the molecular twofold axes by 15° in a way that preserves CRRC interactions, where the two C chains are in different catalytic trimers and are about 120° apart when viewed along the molecular threefold axis.

An indication of the closure of the active site and of the changes in many of the salt links and strong hydrogen bonds is shown schematically in Fig. 6, where domains of catalytic chains C1 and C4 are outlined. The extensive C1-C4 interface of the T form is greatly reduced in the R form. A triple interaction of Glu^{239} of C4 (or C1) with Lys^{164} and Tyr^{165} of C1 (or C4) is broken as the T form goes to the R form; in this same transition an intradomain interaction between Tyr^{240} and Asp^{271} is broken. In the R form new intrasubunit interdomain interactions are formed among Glu^{50}, Arg^{167}, and Arg^{234}. Also, within the aspartate domain new interactions occur between Arg^{229} and Glu^{233} and among Glu^{239}, Lys^{164}, and Tyr^{165} in the R form. There are, of course, many other interactions (*18*) that have not been described here. Mutagenic experiments that involve most of the interactions that have been mentioned are discussed below.

Function of Active Site Residues

Previous chemical modifications have implicated amino acid side chains in catalysis or binding. For example, phenylglyoxal inactivated the enzyme by modifying a single unidentified Arg residue per active site (*19*). Bromosuccinate (*20*) or trinitrobenzene sulfonate (*21*) caused loss of activity by reaction with Lys^{83} and Lys^{84}, whereas pyridoxylation caused inactivation by modifying only Lys^{84} (*22, 23*). Photooxidation of this pyridoxylated enzyme implicated two unidentified His residues (*22*). Besides the ambiguities in identification, these chemical changes often introduced bulky substituents which themselves may cause the inactivation.

Site-directed mutagenesis reduces some of these ambiguities. When Lys^{83} was converted to Gln, the activity was reduced slightly, but when Lys^{84} was changed to Gln, the activity was reduced by a factor of 4000 relative to the wild type (*24*). The replacement of Ser^{52} by the bulky Phe, which probably remained in the phosphate binding site, caused essentially a total loss of activity (*25*). Significantly, the replacement of His^{134} by Ala reduced activity by 20-fold, and substantially increased the aspartate concentration required for half the maximal velocity (*24*).

Preliminary results on site-directed mutants in or near the active site indicate that Arg^{54}, Gln^{137}, Arg^{167}, and Arg^{229} are all required

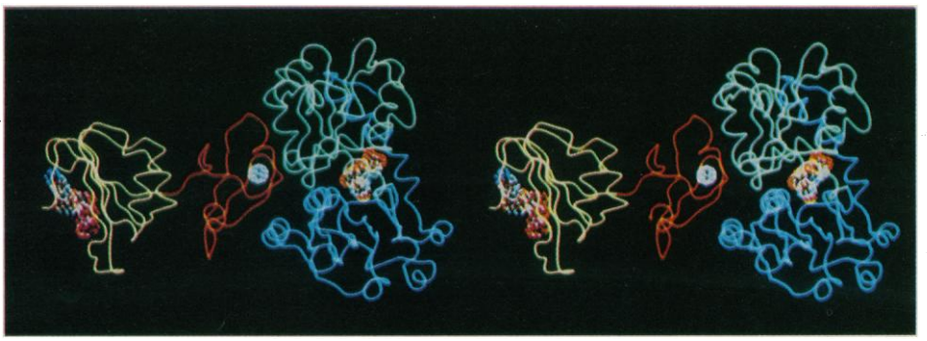

Fig. 3. Stereoview of one catalytic-regulatory pair color coded by the protein domains. The allosteric (yellow) and zinc (red) domains of regulatory chain are toward the left, whereas the aspartate (blue) and carbamyl phosphate (light green) domains of the catalytic chain are toward the right. Shown as dotted features are the bisubstrate analog PALA bound at the active site, between the aspartate and carbamyl phosphate domains of the catalytic chain, CTP bound to the effector site in the allosteric domain of the regulatory chain, and zinc bound to its site in the zinc domain of the regulatory chain. The x-ray data of the PALA-liganded enzyme were used to draw this figure (*15*), and the CTP molecule was then added from the CTP-liganded enzyme (*14*).

for activity (Fig. 7A). In addition, replacement of Arg^{105} by His caused little alteration in catalytic activity, whereas conversion of Arg^{105} to Gln reduced the activity 1000-fold. These results confirmed the location of the active sites in the x-ray diffraction studies. Moreover, the three-dimensional structure of the enzyme and modifications of His^{134} suggest that this residue is important for catalysis. In a complex of the enzyme with carbamyl phosphate and succinate (*17*), if the succinate is replaced by aspartate as a model, the amino group of aspartate is about 4 Å from His^{134}. Hence, a 1 Å movement could allow His^{134} to deprotonate the amino group of aspartate. A minor part of the reaction could also proceed by transfer of a proton from this amino group to the phosphate directly or through another agent such as water. We must emphasize that these mechanistic conclusions have not been proved.

Some further proposals arise from the site-directed mutants at Gln^{137}, Arg^{54}, and Arg^{167}. As noted above, replacement of Gln^{137} by Ala reduced activity, but also reduced the affinity of the enzyme for carbamyl phosphate and, surprisingly, for aspartate. Circular dichroism experiments indicated that the conformational change induced by the binding of carbamyl phosphate in the wild-type enzyme is greatly reduced in this mutant. Since the conformational change induced by carbamyl phosphate enhances the binding of aspartate, the reduction of the conformational change in this mutant thus affects binding of aspartate, as well as of carbamyl phosphate. Turning now to Arg^{54}, which interacts with the anhydride oxygen of carbamyl phosphate, we speculate that this residue promotes the release of phosphate from the tetrahedral intermediate. We also propose that Arg^{167}, which interacts with the α-carboxylate of PALA or succinate, orients aspartate correctly for the true enzymatic reaction. Further mutagenic and three-dimensional structural studies may provide hypotheses for functions of other residues in the catalytic mechanism.

Function of Residues in the Allosteric Transition

In the homotropic transition (in the absence of ATP or CTP), changes in salt links or strong hydrogen bonds occur when substrate analogs induce the T to R transition. We have concentrated our site-specific mutagenesis studies on these interactions. For example, when PALA binds, the closure of the aspartate domain toward the carbamyl phosphate domain is stabilized by interactions among Glu^{50}, Arg^{167}, and Arg^{234}. When Glu^{50} is changed to Gln (Fig. 7B), the mutant has no cooperativity and has greatly reduced affinity for substrates. It appears that these interdomain bridging interactions are critical for the formation of the high-affinity–high-activity conformation of the active site (*26*). When Arg^{234} is replaced by Ser, the mutant has properties similar to the Gln^{50} mutant (Fig. 7B).

The interdomain bridging interactions and the closure of the domains of the catalytic chain are directly related to the geometry of the active site. Using site-directed mutagenesis, we have shown that both Arg^{167} and Arg^{229} are catalytically important residues (see Fig. 7A). Arg^{167} forms a salt link with Glu^{50} as part of the interdomain bridging interactions and is directly bound to PALA in the R state. Furthermore, Glu^{233}, which seems to have no function in the T state, is bound to Arg^{229} in the R state. The conversion of Glu^{233} to Ser results in an enzyme with 80-fold lower activity and reduced affinity for aspartate, suggesting that the function of Glu^{233} is to hold Arg^{229} in the proper orientation for catalysis. Furthermore, the specific interaction between Arg^{229} and Glu^{233} can take place only after the closure of the domains of the catalytic chain; Arg^{105} and Glu^{50} are also involved in a similar type of interaction. In the T state, Arg^{105} is linked to Glu^{50}, but after the domain closure, Arg^{105} is found to interact with the phosphonate portion of PALA, whereas Glu^{50} is involved in the interdomain bridging interactions. Thus the closure of the domains assists in the formation of the active site pocket.

Domain closure alone is not sufficient to orient Glu^{233} correctly for the stabilization of Arg^{229} or to orient Arg^{234} correctly for the establishment of the interdomain bridging interactions. As the comparison of the T and R state structures has revealed, there is a large reorientation of the 240s loop. This loop movement shifts the position of the guanidinium group of Arg^{234}, which is linked to Glu^{50} in the R state, and which is approximately 7.5 Å from its T state position. The rearrangement of this loop is rather complex in that a number of specific interactions are broken and formed by the loop movement. Specifically, the intrachain interaction between Asp^{271} and Tyr^{240} and the intersubunit interactions between Glu^{239} and both Lys^{164} and Tyr^{165} seem to restrain the position of the 240s loop in the T state, whereas the Arg^{229}-Glu^{233} and Glu^{50}-Arg^{234} salt links seem to stabilize the loop in the R state. In order to acquire more details about the function of these interactions, we have used site-directed mutagenesis to perturb them. When Tyr^{240} was replaced by Phe, a substantial reduction in cooperativity and a marked increase in the affinity for aspartate, but no alteration in the specific activity, were observed (Fig. 7B) (*27*). When Asp^{271} was changed to Asn, an enzyme was obtained having almost the identical properties as the enzyme in which Phe was substituted for Tyr^{240}. These results indicate that the interaction between Tyr^{240} and Asp^{271} is important but not critical for the stability of the low-affinity–low-activity T state and is unnecessary for the stability of the R state.

A comparison of the T and R state structures reveals that the intersubunit interactions between Glu^{239} of one catalytic subunit and both Lys^{164} and Tyr^{165} of the other catalytic subunit, which exist in the T state, are completely absent in the R state structure. Based on the structural data, these interactions seem to stabilize the more compact T state. The replacement of Glu^{239} by Gln causes a

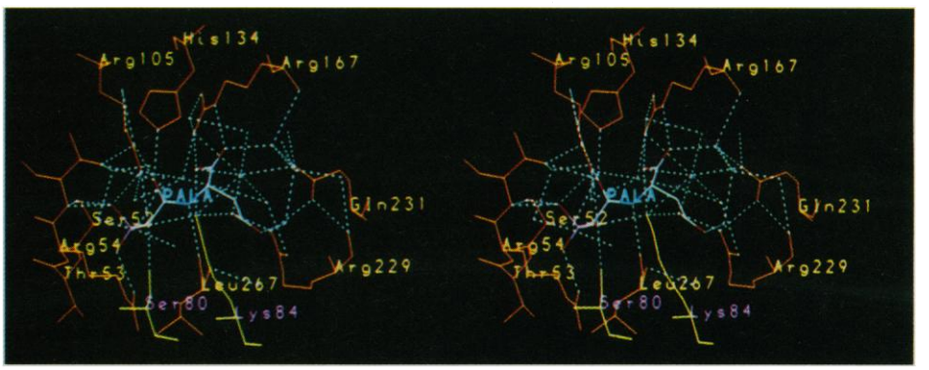

Fig. 4. Stereoview of the PALA binding site in aspartate transcarbamylase. A recent structure of the enzyme with carbamyl phosphate and succinate bound suggests that the terminal phosphate unit and the carboxylate anions of PALA bind to the enzyme in a similar fashion as this substrate and substrate analog pair (*17*). The active site is composed of residues from two adjacent catalytic chains (for example, C1–C2). In this figure all of the side chains that interact with PALA are shown. Those in red come from one catalytic chain while those in yellow (Ser^{80} and Lys^{84}) come from the other catalytic chain. The hydrogen-bonding interactions that stabilize PALA in the active site are also shown as dotted blue lines. Hydrogen bonds that terminate at positions other than the amino acid side chains shown represent hydrogen bonds to water molecules that have been omitted for clarity.

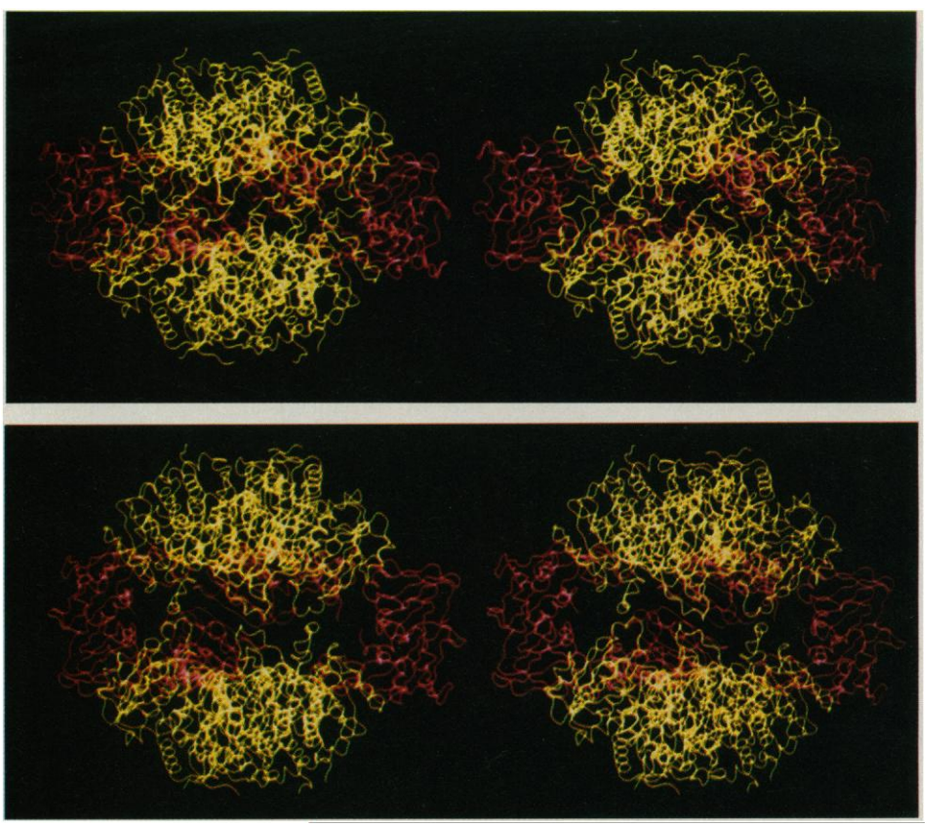

Fig. 5. Stereoviews of the T state (**A**) and R state (**B**) of aspartate transcarbamylase. Data for the T state are from the CTP-liganded structure (*14*) and for the R state from the PALA-liganded structure (*15*). When PALA binds to aspartate transcarbamylase, there is a 12 Å elongation of the molecule along the threefold axis that is accompanied by opposite 5° rotations of each catalytic subunit and a 15° rotation of the regulatory subunits around each of the twofold axes. Additional conformational changes also occur on the tertiary level.

complete lost of cooperativity, no alteration in maximal velocity, and an enhanced affinity for aspartate. Although kinetic experiments suggest that this enzyme is locked in the high-affinity R state, a preliminary x-ray diffraction study shows unit cell changes that suggest a form of the Gln^{239} mutant that is between the T and R forms. These preliminary crystallographic studies have now been confirmed by low-angle x-ray scattering experiments in the laboratory of G. Hervé by P. Vachette using synchrotron radiation at LURE (Laboratory for the Utilization of Electromagnetic Radiation). Detailed three-dimensional x-ray studies are now in progress to further characterize the Gln^{239} mutant enzyme. The kinetic data nevertheless indicate that the simple replacement of Glu^{239} by Gln is sufficient to destabilize the low-affinity–low-activity state, which makes the high-affinity–high-activity state the only form in which this mutant enzyme can exist. Thus the interactions between the catalytic chains of the upper and lower trimer are critical for the stability of the T state. When these links are lost, the enzyme is incapable of remaining in the T state.

The Allosteric Mechanism

Based on the structural data and the results of our site-directed mutagenesis experiments, the following somewhat speculative mechanism is proposed for the allosteric transition (*28*). The binding of the first aspartate molecule (in the presence of carbamyl phosphate) causes two major structural changes in the enzyme. First, a closure of the two domains within a catalytic chain occurs with corresponding shifts in the 80s and 240s loops, thus establishing an active site with high affinity for the substrates and increased catalytic activity. Second, simultaneously with these tertiary changes there is a quaternary conformation change that results in the closure of the domains in all of the other catalytic chains and the conversion of all of the remaining active sites into the high-affinity–high-activity form. Perhaps the most important feature of this mechanism is an intrinsic difference in both substrate affinity and catalytic activity between the T and R states of the enzyme. The binding of substrates at one active site is sufficient to cause all of the remaining active sites

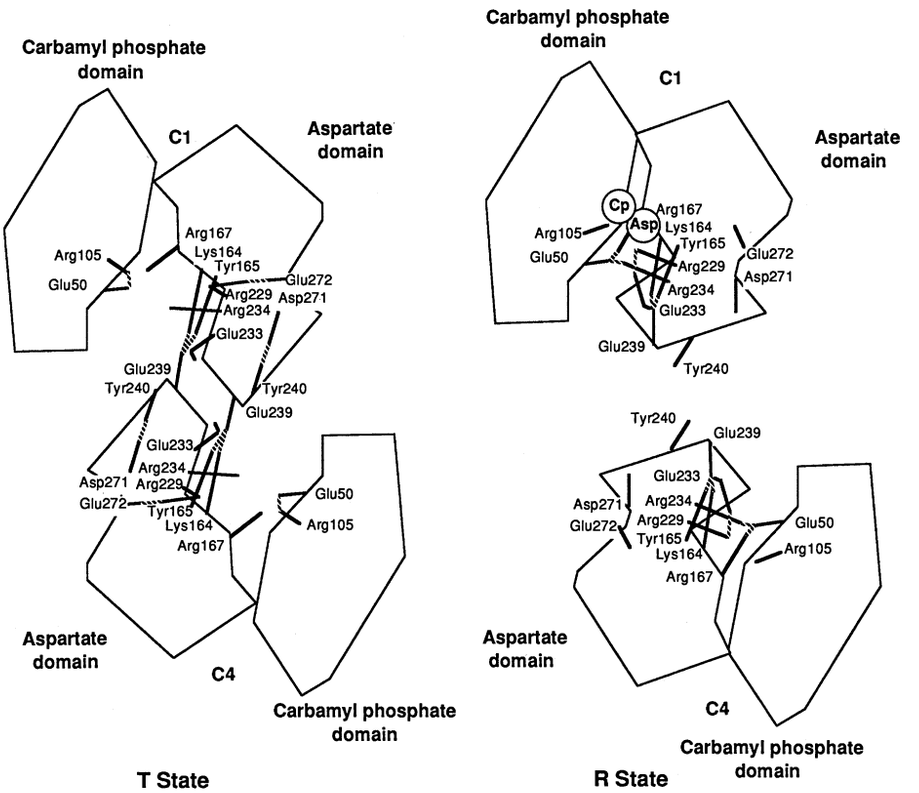

Fig. 6. A model for the mechanism of homotropic cooperativity in aspartate transcarbamylase. Shown schematically are the two extreme conformations of a C1–C4 pair in the T state (**left**) and the R state (**right**), as deduced from x-ray crystallography (*14, 15*). For clarity, only one catalytic chain from each of the upper (C1) and lower (C4) catalytic subunits is shown. Because of the molecular threefold axis, the various interactions shown here are repeated in the C2–C5 and C3–C6 pairs. Upon aspartate binding (in the presence of carbamyl phosphate), the aspartate domain moves toward the carbamyl phosphate domain, which results in the closure of the active site. The 240s loops of C1 and C4 undergo a large alteration in position and change from being side by side in the T state to almost one on top of the other in the R state. On the quaternary level, the catalytic subunits move apart, resulting in an elongation of the molecule. The binding of carbamyl phosphate to the enzyme induces a local conformational change in the enzyme that enhances the binding of aspartate and perhaps causes the loss of the salt link between Glu^{50} and Arg^{105}, which allows Arg^{105} to reorient and bind carbamyl phosphate. The binding of the substrates at one active site induces the domain closure in that catalytic chain and requires a quaternary conformational change that allows the 240s loops of the upper and lower catalytic chains to move to their final positions. As outlined in the text, the quaternary conformational change causes the loss of a whole series of interactions that normally stabilize the constrained T state of the enzyme and results in the formation of the high-activity–high-affinity R state. The formation of the R state, in a concerted fashion, is further stabilized by a variety of new interactions that are both interdomain and intrachain in nature. The various interactions that stabilize these two allosteric states of the enzyme have been observed in the x-ray structures and their functional importance has been deduced by site-directed mutagenesis.

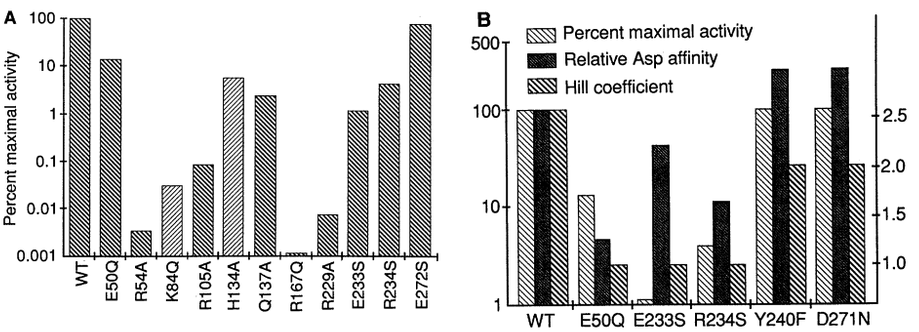

Fig. 7. (**A**) Histogram showing the percent maximal activity for a series of mutant versions of aspartate transcarbamylase. All of the mutant enzymes except for K84Q and H134A (*23*) were created in the laboratory of one of us (E.R.K.). A logarithmic axis is used to depict the variation in activity of these mutant enzymes, which in the worst case approaches a 10^5 reduction in activity. The one-letter amino acid codes are used both to represent the original amino acid, which precedes the substitution site, as well as the new amino acid, which follows the substitution site; WT, wild type (*31*). (**B**) A comparison of the properties of a series of mutants that are important for the stabilization of the two allosteric forms of the enzyme (percent maximal activity and relative Asp affinity, left axis; Hill coefficient, right axis). The interdomain bridging interaction between Glu^{50} and Arg^{234} stabilizes the R state (*26*), whereas the link between Tyr^{240} and Asp^{271} stabilizes the T state (*27*). The salt link between Glu^{233} and Arg^{229} correctly positions the latter residue to interact with the β-carboxylate of aspartate in the R state.

to be converted, in a concerted manner, into a form that has both substantially enhanced affinity for the substrates and catalytic efficiency. Kinetic measurements of the reverse reaction support the requirement for a concerted transition (*29*).

What are the molecular level events that make this mechanism possible? For the wild-type enzyme, there is ample evidence that the allosteric change is induced by the binding of substrates. Substrate binding not only causes tertiary conformational changes within a catalytic chain resulting in the closure of the two domains, but also results in an expansion of the holoenzyme along its molecular threefold axis. The domain closure is a complex structural rearrangement that involves more than a simple hinge motion and that cannot occur without conformational changes at the quaternary level.

The key to the entire quaternary change is the rearrangement of the 240s loop of the aspartate domain. This loop not only undergoes a shift in position due to the movement of the aspartate domain, but also undergoes a major reorientation, which is stabilized by new interdomain and intrachain interactions (see Fig. 6). In the T state, the 240s loop of C1 is maintained far apart from the carbamyl phosphate domain by both the Tyr^{240}-Asp^{271} interaction and the Glu^{239}-Lys^{164} and Glu^{239}-Tyr^{165} links between neighboring 240s loops. These interactions prevent the movement of the 240s loop toward the carbamyl phosphate domain, which would result in a closure of the domains and the formation of the high-affinity–high-activity state through the Glu^{50}-Arg^{167} and Glu^{50}-Arg^{234} salt bridges. In order for domain closure to occur upon aspartate binding, not only must the interactions that stabilize the 240s loop in the T state be broken, but also the steric constraints must be overcome. This steric hindrance is relieved by a structural rearrangement of the loop that ruptures the Tyr^{240}-Asp^{271} interaction and the two symmetrically related links between Glu^{239} and Lys^{164} and Tyr^{165} (C1–C4) resulting in domain closure. However, this change

cannot occur only in one C1–C4 pair, since the different catalytic chains of the upper and lower subunits are in fact held together partly by the favorable interactions between their respective 240s loops. Any changes in the intersubunit interactions of one pair, for example, C1–C4, is transmitted to the C2–C5 and C3–C6 pairs as well. Thus the molecule is converted to the R conformation by the rotations and elongations previously described. The analysis of a double mutant, at both Glu^{50} and Tyr^{240}, supports this model (*28*).

We now consider the C:R interactions in the T and R structures (*14, 15, 30*). A major change occurs in the C1–R4 (that is, C6–R3) interface of the T form; this substantial interface disappears in the more expanded R form. Also, the C1–C4 interface decreases considerably in the T to R transition. Other interfaces such as C1–C2 (C5–C6) and C1–R1 (C6–R6) change by lesser amounts, whereas little change occurs in the R1–R6 interface in the allosteric transition. These interfaces, and the interface between domains of the R chain, have not yet been subjected to extensive single point mutations. The disappearance or decrease of these interfaces as the molecule changes from T to R is probably largely compensated by the binding interactions between enzyme and substrates, including the changes in tertiary structure that bring the two domains of the catalytic chain closer together. Clearly, the active site of the T form is more open than the active site of the R form of the enzyme.

So far we have discussed homotropic cooperativity. The heterotropic effects of inhibition by CTP and of activation by ATP involve the transmission of conformational information some 60 Å from the allosteric site to the nearest active sites (see Fig. 3). Structural and mutagenic studies are currently in progress to identify possible distinct pathways for the heterotropic effects in the regulation of aspartate transcarbamylase.

REFERENCES AND NOTES

1. M. E. Jones, L. Spector, F. Lipmann, *J. Am. Chem. Soc.* 77, 819 (1955); P. Reichard and G. Hanshoff, *Acta Chem. Scand.* **10**, 548 (1956).
2. R. A. Yates and A. B. Pardee, *J. Biol. Chem.* **221**, 757 (1956); J. C. Gerhart and A. B. Pardee, *ibid.* **237**, 891 (1962); *Cold Spring Harbor Symp. Quant. Biol.* **28**, 491 (1963).
3. The holoenzyme consists of the entire aspartate transcarbamylase molecule composed of two catalytic subunits (C_3) and three regulatory subunits (R_2).
4. J. C. Gerhart and H. K. Schachman, *Biochemistry* **4**, 1054 (1965).
5. J. Monod, J. Wyman, J.-P. Changeux, *J. Mol. Biol.* **12**, 88 (1965).
6. D. E. Koshland, Jr., G. Nemethy, D. Filmer, *Biochemistry* **5**, 365 (1966).
7. We use T and R for the structural states. If the high-affinity (HA) or low-affinity (LA) states do not correspond to these structural states, we propose notations such as T_{HA} and R_{LA}.
8. K. D. Collins and G. R. Stark, *J. Biol. Chem.* **246**, 6599 (1971).
9. ———, *ibid.* **244**, 1869 (1969).
10. M. W. Kirshner and H. K. Schachman, *Biochemistry* **10**, 1919 (1971); *ibid.* **12**, 2997 (1973); J. C. Gerhart and H. K. Schachman, *ibid.* 7, 538 (1968).
11. J. H. Griffin *et al.*, *J. Biol. Chem.* **248**, 5057 (1973).
12. M. F. Moody, P. Vachette, A. M. Foote, *J. Mol. Biol.* **133**, 517 (1979).
13. R. B. Honzatko *et al.*, *ibid.* **160**, 219 (1982); H.-M. Ke, R. B. Honzatko, W. N. Lipscomb, *Proc. Natl. Acad. Sci. U.S.A.* **81**, 4027 (1984).
14. R. B. Honzatko and W. N. Lipscomb, *J. Mol. Biol.* **160**, 265 (1982); K. H. Kim, Z. Pan, R. B. Honzatko, H.-M. Ke, W. N. Lipscomb, *ibid.* **196**, 853 (1987).
15. K. L. Krause, K. W. Voltz, W. N. Lipscomb, *Proc. Natl. Acad. Sci. U.S.A.* **82**, 1643 (1985); K. W. Voltz, K. L. Krause, W. N. Lipscomb, *Biochem. Biophys. Res. Commun.* **136**, 822 (1986); K. L. Krause, K. W. Voltz, W. N. Lipscomb, *J. Mol. Biol.* **193**, 527 (1987).
16. E. A. Robey and H. K. Schachman, *Proc. Natl. Acad. Sci. U.S.A.* **82**, 361 (1985); S. R. Wente and H. K. Schachman, *ibid.* **84**, 31 (1987).
17. E. Gouaux and W. N. Lipscomb, *ibid.* **85**, 4205 (1988).
18. H.-M. Ke, W. N. Lipscomb, Y. Cho, R. B. Honzatko, *J. Mol. Biol.*, in press.
19. E. R. Kantrowitz and W. N. Lipscomb, *J. Biol. Chem.* **251**, 2688 (1976).
20. A. M. Lauritzen and W. N. Lipscomb, *ibid.* **257**, 1312 (1982).
21. R. S. Lahue and H. K. Schachman, *ibid.* **259**, 13906 (1984).
22. P. Greenwell, S. L. Jewett, G. R. Stark, *ibid.* **248**, 5994 (1973).
23. T. D. Kempe and G. R. Stark, *ibid.* **250**, 6861 (1975).
24. E. A. Robey *et al.*, *Proc. Natl. Acad. Sci. U.S.A.* **83**, 5934 (1986).
25. H. K. Schachman *et al.*, *ibid.* **81**, 115 (1984).
26. M. M. Ladjimi *et al.*, *Biochemistry* **27**, 268 (1988).
27. S. A. Middleton and E. R. Kantrowitz, *Proc. Natl. Acad. Sci. U.S.A.* **83**, 5866 (1986).
28. M. M. Ladjimi and E. R. Kantrowitz, *Biochemistry* **27**, 276 (1988).
29. J. Foote and W. N. Lipscomb, *J. Biol. Chem.* **256**, 11428 (1981); J. Foote and H. K. Schachman, *J. Mol. Biol.* **186**, 175 (1985).
30. J. Cherfils, thesis, Universite Paris-Sud, Orsay, France (1987).
31. Abbreviations for the amino acid residues are: A, Ala; C, Cys; D, Asp; E, Glu; F, Phe; G, Gly; H, His; I, Ile; K, Lys; L, Leu; M, Met; N, Asn; P, Pro; Q, Gln; R, Arg; S, Ser; T, Thr; V, Val; W, Trp; and Y, Tyr.

32. This work was supported by a grants from the National Institutes of Health (GM26237 to E.R.K. and GM 06920 to W.N.L.); E.R.K. also thanks the Camille and Henry Dreyfus Foundation for a fellowship.

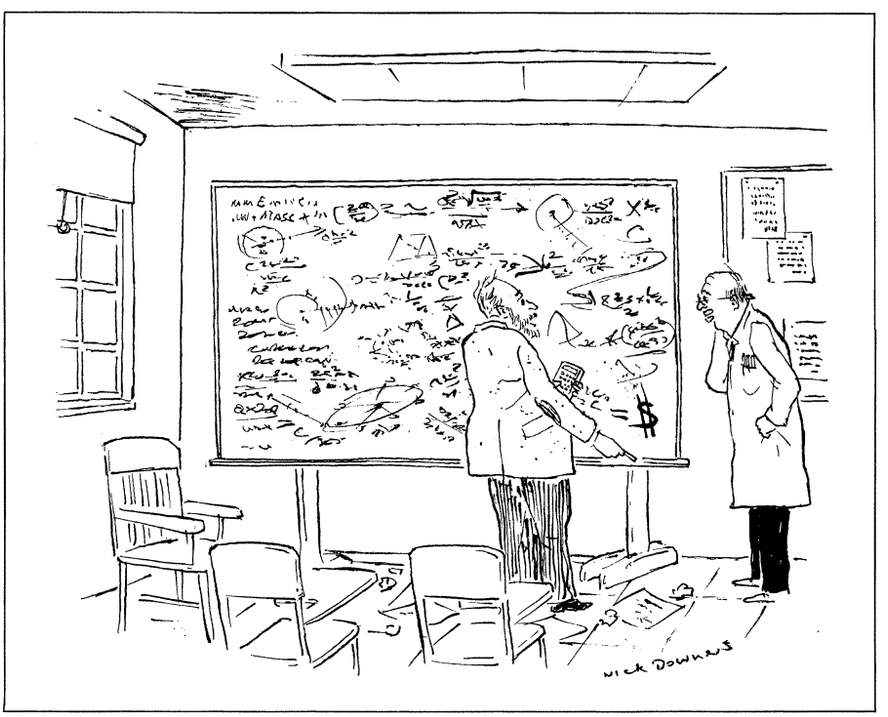

"That's it, then – Time is Money."